Wave-front Aberrations of Laser Beams Propagating through the Atmosphere

Nurdan Anilmiş Baci, Aydin Yeniay

Wave-front Aberrations of Laser Beams Propagating through the Atmosphere

Nurdan Anılmış Baci*[a], Aydın Yeniay[a]
[a]TÜBİTAK BILGEM National Research Institute of Electronics and Cryptology, Kocaeli, Turkey

ABSTRACT

Small temperature variations carried by the turbulent velocity field in the Earth's atmosphere produce small phase perturbations in laser beam propagating through it. Perturbations in the phase cause wave-front errors and may significantly decrease the Strehl ratio of the laser beam. For compensation of atmospheric distortions, adaptive optics systems are used. Before the design of any adaptive optics system, the simulation of the atmospherically distorted laser beam is important. In this work, we describe the purpose, theory, implementation, and results of a wave optics propagation simulation code LAtmoSim and we investigate the effect of laser system parameters on the degree of the wave-front error caused by turbulence.

Keywords: atmospheric turbulence, wave-front aberrations, laser beam propagation

1. INTRODUCTION

Laser beams that are used in directed energy and free-space optical communication applications can become severely distorted by optical turbulence when propagating through the atmosphere. Those distortions mostly originate in the atmospheric boundary layer, which typically extends up to a height of about 2 kilometers and contains 75% percent of the atmosphere's mass. Effects are beam wander, beam broadening and irradiance fluctuations. The use of adaptive optics techniques is possible to mitigate the effects of turbulence and such systems are well known for astronomical applications but implementation and performance in directed energy applications are still not very well known. Any AO system's goal is to eliminate the distortions in the wave-front of the light that is the result of optical path variations through measuring the errors using a wave-front sensor, calculating an appropriate correction, and applying this correction to a deformable mirror. This feedback loop is carried out several hundred times a second to comply with the temporal bandwidth requirement. To determine the characteristics of an AO system, the effects of the atmospheric turbulence on the wave-front has to be simulated. The estimation of the performance of laser systems depends on the accuracy of the atmospheric models being used in the propagation prediction codes. After decades of research, some analytical theories such as geometrical optics[1], Rytov Method and Markov approximation[2-4] have been developed to calculate the characteristics of laser beam propagation. But these methods are approximation in certain conditions, therefore their applicability is limited and theoretical calculations of the statistics of scintillation are difficult especially when the intensity fluctuations become large. Therefore, numerical methods are developed to get a more realistic representation of atmospheric turbulence effects on laser beam propagation. These methods are known as beam propagation method[5]. Other names for the methods are the split-step Fourier technique[6] and the random phase-screen method[7, 8]. Here we introduce laser beam propagation code LAtmoSim which enables us to assess the effect of the atmosphere on the laser beam wave-front and to determine the design parameters of the AO system by using methods described above. In this paper, we also present the results from the work done to predict the intensity of the atmospheric turbulence. A quantitative measure of the intensity of optical turbulence is called the refractive index structure parameter, C_n^2. The measurement of C_n^2 is difficult; it requires expensive and bulky detectors and optical imaging systems. Estimating boundary layer C_n^2 from easily available meteorological parameters, such as temperature and humidity makes to predict the effectiveness of a laser system before its use easy.

The remainder of the paper is organized as follows. Section 2 introduces the capabilities of the simulation software LAtmoSim. Section 3 describes the basic mathematical models used for simulation operations such as the phase screen model. Section 4 presents the results of the work done to predict the refractive index structure parameter. In Section 5, models of wave-front aberrations are explained. In Section 6, we conclude with the prospect of how this work might be extended.

*nurdan.baci@tubitak.gov.tr; phone 90 262 675-2335; fax 90 262 675-2119; www.tubitak.gov.tr

2. LATMOSIM: SIMULATIONS OF LASER BEAM PROPAGATION THROUGH THE ATMOSPHERE

LAtmoSim is developed to do numerical calculations on laser beam propagation through the atmosphere. The software is written in Python and Tkinter is used to develop the user interface of the software. The code takes into account atmospheric effects such as absorption, scattering, turbulence and thermal blooming. Including effects of aerosol and molecular absorption and scattering of radiation is achieved by providing a user interface for parameters in FASCODE. As an alternative to FASCODE, LAtmoSim calculates atmospheric transmittance by utilizing data fitted analytic models of visibility and rain[9, 10]. For slant path engagement scenarios such as ground to air and air to ground, it uses the Hufnagel-Valley model for vertical C_n^2 profiles. LAtmoSim can create multiple numbers of focused or collimated Gaussian, super-Gaussian and Bessel Gaussian laser beams with properties including wavelength, beam size, truncation ratio, beam quality M^2, total power, and super-Gaussian order and Bessel coefficient. Atmospheric turbulence is modeled by generating random phase screens and filtering with the Kolmogorov spectrum. The loss of low spatial frequencies is handled with the sub-harmonic method. Those methods are described in detail in Section 3. The code calculates ensemble averages with a large number of realizations for the calculation of beam wander, long-term spot size, on-axis scintillation index SI; and compares those simulation results with values obtained from analytical calculations from Rytov theory. The code may be run both wave optics and geometric propagation mode to allow the code to be checked against linear analytical models. The other calculations include power-in-the-bucket, tracked-beam Strehl ratio, RMS wave front error, Peak to Valley (PtV) value of the phase distribution.

In addition to atmospheric turbulence, a high-energy beam introduces an entirely new physical effect: Thermal blooming. Thermal blooming is the spreading of a laser beam when the beam heats the medium through which it is propagating. As the laser beam passes through the atmosphere, some of the beam's energy is absorbed, heating the atmosphere. The heated region will be less dense and will, consequently, have a lower index of refraction. Since the hottest regions will normally be in the center of the beam, a negative lens will develop in the atmosphere, and this lens will cause the divergence of the beam. LAtmoSim has both analytical[11] and numerical steady-state model[12] of thermal blooming. Figure 1 shows the results of two different atmospheric cases. In the first case, we take into consideration only the turbulence. In the second case, we added the effect of thermal blooming to turbulence. The simulation parameters are given in Table 1. The short term spots for each case are seen in Figure 1.

Table 1: Simulation parameters

Beam Parameters		Atmosphere parameters	
Initial beam size	10 cm	Distance	5 km
Beam quality	2	C_n^2	1.0e-14 $m^{-1/3}$
Wavelength	2141 nm	Transverse wind speed	4 m/s
Power	10 kW	Absorption coefficient	1.0e-4 1/m

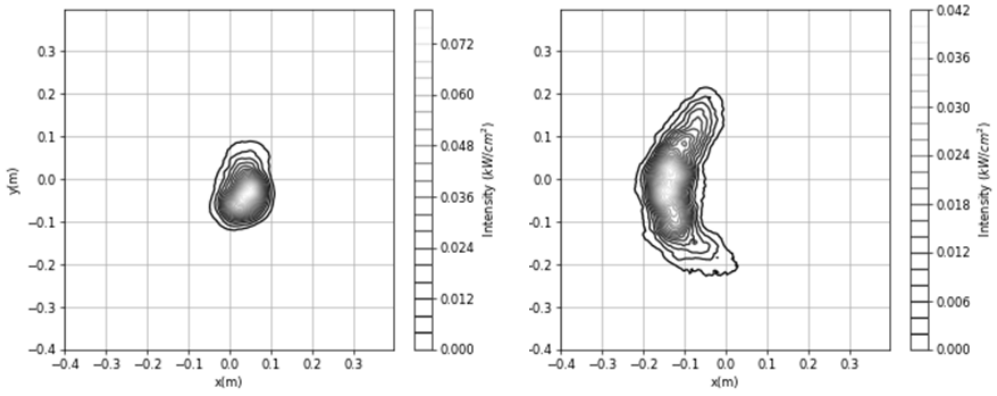

Figure 1: Gaussian beam propagation in LAtmoSim left: only with turbulence, right: turbulence and thermal blooming

3. ATMOSPHERIC TURBULENCE MODELING

Turbulence is a complex phenomenon, and characterizing and modeling its effect on optical propagation poses a significant challenge. Both analytical[13-16] and numerical[17, 18] methods have been developed. A promising method of

numerical simulation uses a split-step phase screen approach. The fluctuations in refractive index are very small and their scale size is very large compared to the wavelength of the light, diffraction and scattering can be separated in numerical calculations. The propagation path is divided into many short intervals so that the propagating wave is hardly disturbed by each interval, but their cumulative effect can be significant. The starting point of numerical models is the parabolic approximation to the wave equation where the continuous random media is treated as a series of random phase screens transverse to the propagation direction of the electric field E. The field is propagated between the phase screens using the numerically efficient fast-Fourier-transform (FFT) algorithm. Random phase screens are generated with a spectral-domain algorithm also based on the FFT. Generation of random phase screens φ(x, y) is accomplished by[17]

$$\varphi(j\Delta x, l\Delta y) = \sum_{n=0}^{N_x}\sum_{m=0}^{N_y}\left[a(n,m) + ibz(n,m)\right]\times\exp\left[2\pi i(jn/N_x + lm/N_y)\right] \quad (1)$$

Where Δx and Δy are the grid spacing in the x and y coordinates, respectively; N_x and N_y are the array dimensions; $L_x = \Delta x\, N_x$ and $L_y = \Delta y\, N_y$ are the linear dimensions; and a (n, m) and b (n, m) are zero-mean Gaussian uncorrelated random numbers with

$$\left\langle a^2(n,m)\right\rangle = \left\langle b^2(n,m)\right\rangle = \Delta q_x \Delta q_y \Phi_\varphi(n\Delta q_x, m\Delta q_y) \quad (2)$$

Where <> denotes ensemble average, $\Phi_\varphi(q_x, q_y)$ is the spatial spectrum of the phase screens as a function of propagation distance z, $\Delta q_x = 2\pi / (N_x \Delta x)$ and $\Delta q_y = 2\pi / (N_y \Delta y)$ are the grid size of the simulation in spectral space. The phase spectrum is

$$\Phi_\varphi = 2\pi k^2 \Delta z \Phi_n \quad (3)$$

Where $k = 2\pi / \lambda$ is the wavenumber of the field, Δz is the separation between phase screens in the propagation direction z, and Φ_n is the spectrum of refractive-index fluctuations. The Kolmogorov model is the most frequently used for turbulence description because of its relative mathematical simplicity and good agreement with experiment[19]. Kolmogorov model of the index of refraction power spectrum is

$$\Phi_n(q) = 0.33 C_n^{\,2} q^{-11/3} \quad (4)$$

Where q is the magnitude of three-dimensional wave vector and C_n^2 is the refractive-index structure constant.
Because the phase screens produced by the FFT algorithm are periodic, the simulation of the fields has errors for those statistics that are sensitive to large-scale turbulent fluctuations. These errors will be removed by an improved simulation algorithm for the phase screens. The simulation algorithm does not include the power in the spectral region $(-\Delta q_x/2, \Delta q_x/2)$ and $(-\Delta q_y/2, \Delta q_y/2)$ which produces an error in the large-scale phase fluctuations. Lane et al.[20] proposed an algorithm based on the addition of sub-harmonics with random complex amplitudes to improve the large scale statistics i.e.,

$$\varphi_{SH}(j\Delta x, l\Delta y) = \sum_{p=1}^{N_p}\sum_{n=-1}^{1}\sum_{m=-1}^{1}\left[a(n,m,p) + ib(n,m,p)\right]\times\exp\left[2\pi ijn/(3^p N_x) + 2\pi i lm/(3^p N_y))\right] \quad (5)$$

$$\left\langle a^2(n,m,p)\right\rangle = \left\langle b^2(n,m,p)\right\rangle = \Delta q_{xp}\Delta q_{yp}\Phi_\varphi(n\Delta q_{xp}, m\Delta q_{yp}) \quad (6)$$

If $n \neq 0$ and $m \neq 0$. Here, $\Delta q_{xp} = \Delta q_x / 3^p$ and $\Delta q_{yp} = \Delta q_y / 3^p$ are the spectral domain grid sizes for sub-harmonic order p.
The FFT sub-harmonic phase-screen simulation is no longer periodic and the discontinuities of the phase at the edges of the simulation may produce additional errors. These errors are negligible for beam-wave simulations if the beam is located at the center of the simulation. In Figure 2, phase screens with and without high-frequency components are shown.

In the following example, we explore the impact of the transmitting beam size on the far-field intensity calculated by LAtmoSim. For an atmospheric turbulence condition where the Fried radius is equal to 6 cm, we propagate several collimated beams with an ideal Gaussian shape. The beam diameters are chosen; 1cm < r_0, 6 cm = r_0, and 20cm > r_0. The propagation distance used in this simulation is 2 km. Figure 3 shows the resulting intensity profiles for each beam. Beam with a diameter equal to the Fried parameter seems to be the least affected by turbulence.

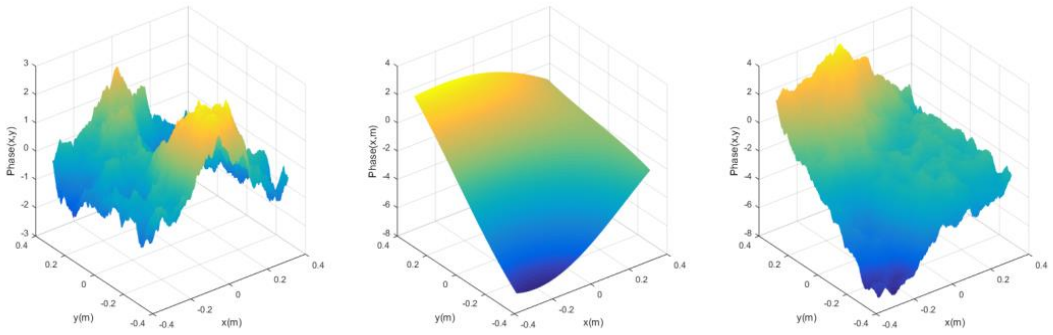

Figure 2: Phase screen with only high-frequency component (left), the low frequency component of the phase created by using the sub-harmonic method (middle) and the total phase screen (right)

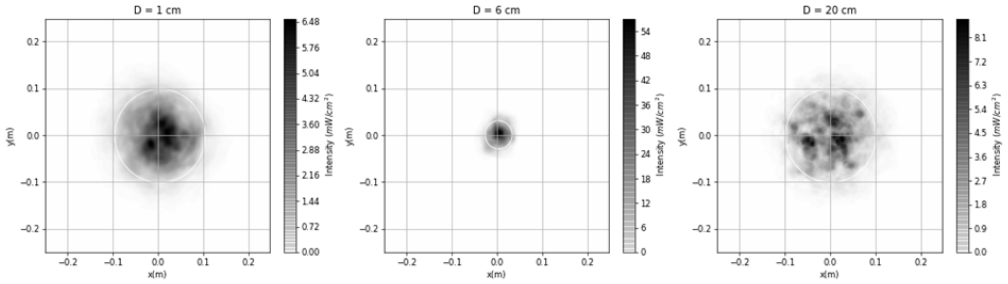

Figure 3: The intensity patterns of collimated beams with different beam sizes w_0 = 5 mm, 3 cm and 10 cm passing through an atmosphere with r0 = 6 cm are shown.

4. C_N^2 PREDICTION MODELS

We made simultaneous measurements of C_n^2 and other atmospheric parameters that are known causing boundary layer turbulence. From the analysis of C_n^2 data gathered from scintillometer measurements and meteorological data, we found that net radiation of the atmosphere, relative humidity, and wind to be the atmospheric parameters that are most correlated with C_n^2. Unfortunately, net radiation data is also not easily available. Therefore, we used Holtslag model[21] which uses the time of the year, latitude, longitude, temperature, cloud cover and albedo as variables to calculate the net radiation. We compared net radiation data from pyrradiometer measurements with the Holtslag model for clear sky conditions and we found quite good agreement between the two (Figure 4).

Next, we used artificial neural networks to have C_n^2 as a function of net radiation, relative humidity, and wind speed. Approximately six months of data from measurements of C_n^2, net radiation, relative humidity, and the wind is used as a training set. Later, a user-interface for the C_n^2 estimator is developed which allows users to predict C_n^2 from date, time, latitude, longitude, temperature, relative humidity, wind speed, cloud cover, albedo and height from the ground level. In Figure 5, a comparison of estimated and measured C_n^2 values for the 24-hour duration is shown.

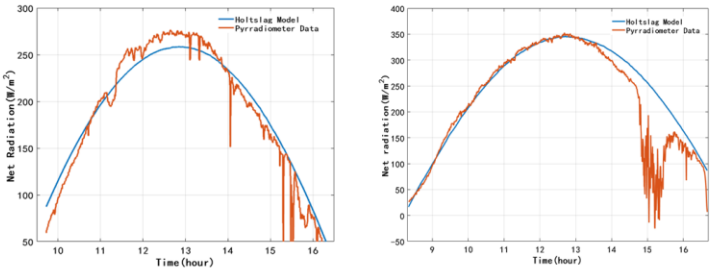

Figure 4: Holtslag model comparison with data

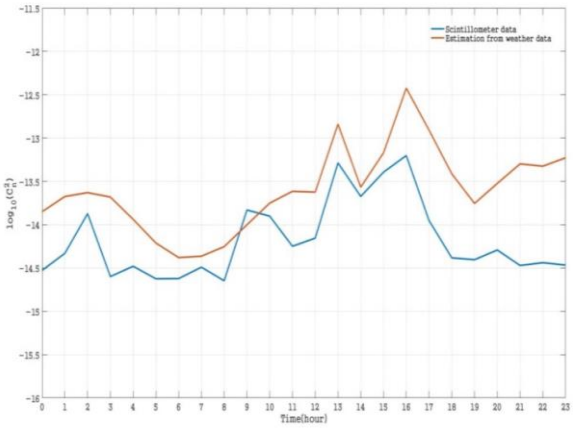

Figure 5: Comparison of estimated and measured C_n^2 values

5. MODELING OF WAVEFRONT ABERRATIONS

The performance of an AO system can be evaluated using several different metrics. The most common performance metric for AO is the wave-front error variance. By minimizing the variance of wave-front error σ_φ^2, according to following Marechal approximation

$$S = \exp(-\sigma_\varphi^{\ 2}) \tag{7}$$

It is possible to maximize Strehl ratio S. The use of Zernike polynomials for describing the aberrations of atmospheric turbulence is well known[22]. Beam wander is related to tip and tilt aberrations which are the second and third term of Zernike polynomials. Higher-order terms are the result of scintillation. Far-field phase distribution of a laser beam passing through atmospheric turbulence can be calculated by numerical propagation methods described in Section 3. If we let φ(x, y) be a turbulence-induced phase distribution, we can decompose this function over an orthogonal set of Zernike polynomials $Z_i(x, y)$

$$\varphi(x, y) = \sum_{i=0}^{\infty} a_i Z_i(x, y) \tag{8}$$

Using cross-correlations of Zernike coefficients of turbulent phase with Kolmogorov statistics, Noll[22] deduced that residual wave-front error for piston removed and tip-tilt removed are respectively

$$\Delta_1 = 1.0299(D/r_0)^{5/3}, \Delta_2 = 0.582(D/r_0)^{5/3}, \Delta_3 = 0.134(D/r_0)^{5/3} \tag{9}$$

Where r_0 is the Fried parameter and D is the receiving aperture diameter. At first, LAtmoSim calculates Zernike coefficients a_i by using the least square method. The accuracy of the least square method is shown in Figure 6.

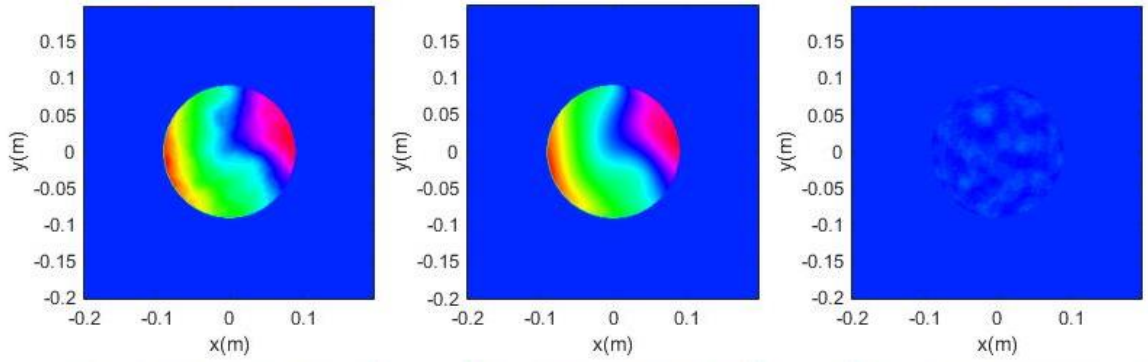

Figure 6: Reconstruction of the phase by Zernike polynomials with 37 modes

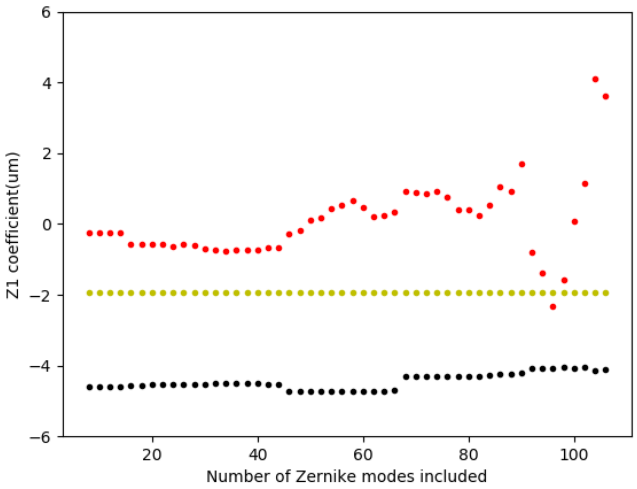

Figure 7: The change observed in the Z1 coefficient as the number of Zernike terms added in the calculations at different sampling values; 128(red), 256(black) and 512(yellow)

We also tested the numerical stability of Zernike coefficients against the changing the number of Zernike terms included in the calculations. Although Zernike polynomials form an orthogonal and complete set in the continuous domain, in discrete numerical calculations to have orthogonal and complete set one has to increase the number of sampling. Figure 7 shows that the stability of the Zernike tilt coefficient increases with an increased sampling number. We conclude that we need to increase the sampling size to 512 to have the correct Zernike coefficients. On the other hand, the Gram Schmidt orthogonalization scheme exists as a solution for the stability problem[23].

After finding Zernike coefficients, the total wave-front error in the first J modes is deduced by using Noll's formula

$$\sigma_J^{\,2} = \sum_{j=1}^{J} < \left| a_j \right|^2 > \tag{10}$$

This allows us to determine how many modes are needed to be corrected to achieve Strehl ratios close to the diffraction-limited performance.

In Figure 8, we see the result of the simulation run for a laser beam with a transmitter aperture size of 12 cm focused at a distance of L=1000 m passing through various atmospheric turbulence conditions. For the simulation, the physical size of the computational grid was set to 0.8 m for both transverse directions and the resolution of the grid was 512 x 512. This corresponds to approximately 1.5 mm pixel size. In the computational domain, pixel size determines the inner scale; l_0 of atmospheric turbulence. For the case where C_n^2 is equal to 1.0e-15 $m^{-2/3}$, the Strehl ratio increases from 0.25 to 0.65 with the correction of only the first two modes; tip and tilt.

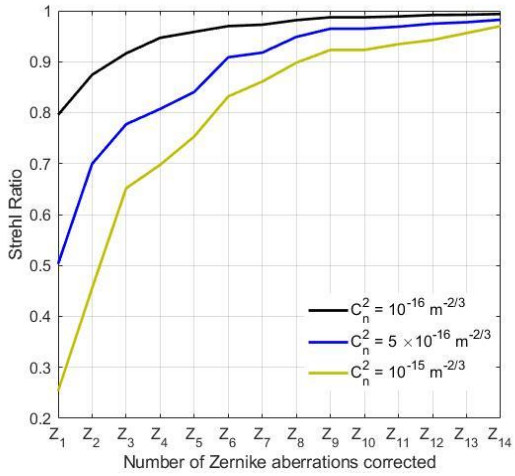

Figure 8: Strehl ratio calculated after correction of each mode

The number of modes corrected is roughly proportional to the number of actuators a deformable mirror used in an AO system has. With the Strehl ratio calculations, we can determine the number of actuators needed for the compensation of atmospheric errors for different engagement scenarios for an ideal AO system. Another important design parameter for DM is stroke; dynamic range of the mirror. The stroke value depends on the PtV of the turbulent phase map. Conventional adaptive optics (AO) systems perform adequately when the phase of a distorted wave-front is continuous across the aperture, which occurs when the turbulence is weak. However, when an optical field is propagated through strong turbulence, it experiences nulls in its amplitude leading to branch points in the phase. It is shown by Fried[24] that when branch points are present in the phase of a turbulence-distorted optical field, the ability of an adaptive optics system to sense all of the perturbations is limited. Because in the case of strong turbulence where the value of Rytov number exceeds 0.3, phase values larger than 2π wrapped to the principal-values which are confined to the range $[-\pi, \pi]$, unwrapping of the phase is required to be able to obtain true PtV and RMS wave-front error. We used the software package[25] which contains a robust phase unwrapping algorithm based on the transport of intensity equation. The aberration coefficients of the unwrapped phase corresponding to different C_n^2 values are calculated. The resulting RMS wave front error and PtV values are shown in Table 2.

Table 2: RMS and peak-to-valley values of wave-front error calculated for different levels of atmospheric turbulence

$C_n^2(m^{-2/3})$	RMS(μm)	PtV(μm)
1.0e-15	0.02	1.1
1.0e-14	0.24	2.1
1.0e-13	1.19	6.2
2.0e-13	2.09	9.8

6. CONCLUSIONS

In this work, we aimed to determine the design parameters of the AO system that are related to the atmospheric turbulence. We calculated the PtV and RMS wave front errors in the beam for different atmospheric turbulent conditions. Our plan includes making experiments that measure the wave-front errors of the laser beam traveling through the atmosphere and compare measurement results with the results obtained from the simulations.

REFERENCES

[1] Clarke, R. H., "Analysis of Laser Beam Propagation in a Turbulent Atmosphere," AT&T Technical Journal, Vol. 64, No. 7 (1985).

[2] Klyatskin, V. I., Kon, A. I., "On the Displacement of Spatially-Bounded Light Beams in a Turbulent Medium in the Markovian-Random-Process Approximation," Radiophysics, Quantum Electronics, 15, 1056-1061 (1972).

[3] Kon, A. I., Mironov, V. L., Nosov, V. V., "Dispersion of Light Beam Displacements in the Atmosphere with Strong Intensity Fluctuations," Radiophysics. Quantum Electronics, 19, 722-725 (1976).

[4] Mironov, V. L., Nosov, V. V., "On the Theory of Spatially Limited Light Beam Displacements in a Randomly Inhomogeneous Medium," J. Opt. Soc. Am. 67, 1073-1080 (1977).

[5] Van Roey, J., van der Donk, J., Lagasse, P. E., "Beam-Propagation Method: Analysis and Assessment," J. Opt. Soc. Amer., 71, No. 7 (1981)

[6] Tappert, F. D., "The Parabolic Approximation Method," in Wave Propagation in Underwater Acoustics (Lecture Notes in Physics, No. 70), J. B. Keller and J. Papadakis, eds., New York: Springer (1977)

[7] Fejer, J. A., "The Diffraction of Waves in Passing through an Irregular Refracting Medium," Proc. Roy. Soc. A, 220, 455-71 (1953)

[8] Lee, R. W., Harp, J. C., "Weak Scattering in Random Media, With Applications to Remote Probing," Proc. IEEE, 57, No. 4, 375-406 (1969)

[9] Marshall, J. S., Palmer, W. "The Distribution of Raindrops with Size", J. Of Meteor., 5, 165-166 (1948)

[10] Kim, I., McArthur, B., Korevaar, E. J., "Comparison of Laser Beam Propagation at 785 nm and 1550 nm in Fog and Haze for Optical Wireless Communications," Proc. of SPIE, 4214 (2001)
[11] Gebhardt F. G., Smith D. C., "Self-Induced Thermal Distortion in the Near Field for a Laser Beam in a Moving Medium", Journal of Quantum Electronics, Vol. QE-7, No. 2 (1971)
[12] Fleck, J. A., Morris, J. R., Feit, M. D., "Time-Dependent Propagation of High Energy Laser Beams through the Atmosphere", Appl. Phys., Vol. 10, 129-160, (1976)
[13] Frisch, U., "Wave propagation in random media," in Probabilistic Methods in Applied Mathematics, A. T. Bharucha-Reid, Ed. Academic Press Inc., New York, 1968, vol. 1, pp. 75–198.
[14] Ishimaru, A., "Wave propagation and scattering in random media," Academic, New York, 1978.
[15] Flatte, S. M., "Sound transmission through a fluctuating ocean," Cambridge University Press, Cambridge, 75–198 (1979)
[16] Rytov, S. M., Kravtsov, V. A., Tatarskii, V. I. "Principles of statistical radio physics: wave propagation through random media," Springer, Berlin (1988)
[17]Frehlich, R., "Simulation of laser propagation in a turbulent atmosphere," Applied Optics, Vol. 39, No. 3, (2000).
[18] Martin, J. M., Flatte, S. M., "Intensity images and statistics from numerical simulation of wave propagation in 3-d random media," Applied Optics, vol. 27, 2111–2125 (1988)
[19] Kolmogorov, A., "Dissipation of energy in locally isotropic turbulence," Turbulence: Classic Papers on Statistical Theory, Wiley-Inter-science, (1961).
[20] Lane, R. G., Glindemann, A., Dainty, J. C., "Simulation of a Kolmogorov phase screen," Waves Random Media 2, 209–224 (1992)
[21] Holtslag, A. A., M., Van Ulden, A. P., "A Simple Scheme for Daytime Estimates of the Surface Fluxes from Routine Weather Data," Journal of Climate and Applied Meteorology, Vol. 22, No. 4 (1983)
[22] Noll, R. J., "Zernike Polynomials and Atmospheric Turbulence", J Opt. Soc. Am, Vol. 66, No. 3(1976)
[23] Upton, R., Ellerbroek, B., "Gram–Schmidt orthogonalization of the Zernike polynomials on apertures of arbitrary shape", Optics Letters, Vol. 29, No. 24, (2004)
[24] Fried, D. L. "Branch point problem in adaptive optics", OSA, Vol. 15 No. 10 (1998)
[25]Zhao, Z, "Robust 2D Phase Unwrapping Algorithm Based on the Transport of Intensity Equation", Measurement Science and Technology, Vol. 30, No. 1(2018)